

DTIC FILE COPY

2

GL-TR-90-0093

AN ASSESSMENT OF THE APPLICATION OF *IN SITU* ION-DENSITY DATA
FROM DMSP TO MODELING OF TRANSIONOSPHERIC SCINTILLATION

AD-A224 392

James A. Secan
Lee A. Reinleitner
Robert M. Bussey
Northwest Research Associates, Inc.
P.O. Box 3027
Bellevue, Washington 98009

DTIC
ELECTE
JUL 30 1990
S D & D

15 March 1990

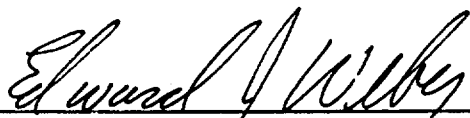
Final Report
15 September 1989 - 14 March 1990

Approved for public release; distribution unlimited

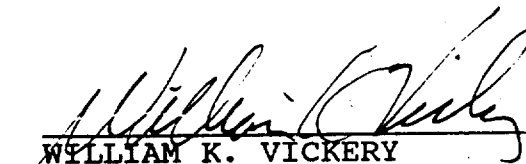
Prepared for:

GEOPHYSICS LABORATORY
AIR FORCE SYSTEMS COMMAND
UNITED STATES AIR FORCE
HANSCOM AFB, MASSACHUSETTS 01731-5000

"This technical report has been reviewed and is approved for publication"



EDWARD J. WEBER
Contract Manager



WILLIAM K. VICKERY
Branch Chief

FOR THE COMMANDER



ROBERT A. SKRIVANEK
Division Director

This report has been reviewed by the ESD Public Affairs Office (PA) and is releasable to the National Technical Information Service (NTIS).

Qualified requestors may obtain additional copies from Defense Technical Information Center. All others should apply to the National Technical Information Service.

If your address has changed, or if you wish to be removed from the mailing list, or if the addressee is no longer employed by your organization, please notify GL/IMA Hanscom AFB, MA 01731. This will assist us in maintaining a current mailing list.

Do not return copies of this report unless contractual obligations or notice on a specific document requires that it be returned.

REPORT DOCUMENTATION PAGE

1a. REPORT SECURITY CLASSIFICATION Unclassified			1b. RESTRICTIVE MARKINGS	
2a. SECURITY CLASSIFICATION AUTHORITY			3. DISTRIBUTION/AVAILABILITY OF REPORT Approved for public release. Distribution unlimited.	
2b. DECLASSIFICATION/DOWNGRADING SCHEDULE				
4. PERFORMING ORGANIZATION REPORT NUMBER(S) NWRA-CR-90-R060			5. MONITORING ORGANIZATION REPORT NUMBER(S) GL-TR-90-0093	
6a. NAME OF PERFORMING ORGANIZATION Northwest Research Assoc. Inc.		6b. OFFICE SYMBOL (if applicable) CR		7a. NAME OF MONITORING ORGANIZATION Geophysics Laboratory
6c. ADDRESS (City, State, and ZIP Code) P.O. Box 3027 Bellevue, WA 98009			7b. ADDRESS (City, State, and ZIP Code) Hanscom AFB, MA 01731-5000	
8a. NAME OF FUNDING/Sponsoring ORGANIZATION		8b. OFFICE SYMBOL (if applicable)		9. PROCUREMENT INSTRUMENT IDENTIFICATION NUMBER F19628-86-C-0195
8c. ADDRESS (City, State, and ZIP Code)			10. SOURCE OF FUNDING NUMBERS	
			PROGRAM ELEMENT NO. 62101F	PROJECT NO. 4643
			TASK NO. 09	WORK UNIT ACCESSION NO. AI
11. TITLE (Include Security Classification) An Assessment of the Application of In situ Ion-density data from DMSP to modeling of Transionospheric Scintillation				
12. PERSONAL AUTHOR(S) Secan, James A., Lee A. Reinleitner, Robert M. Bussey				
13a. TYPE OF REPORT Final Report		13b. TIME COVERED FROM 8 Sep 15 TO 20 Mar 14		14. DATE OF REPORT (Year, Month, Day) 1990 March 15
15. PAGE COUNT 32				
16. SUPPLEMENTARY NOTATION				
17. COSATI CODES			18. SUBJECT TERMS (Continue on reverse if necessary and identify by block number)	
FIELD	GROUP	SUB-GROUP		
04	0		Ionosphere, Ionospheric Scintillation, Radiowave Scintil-	
20	14		lation, Defense Meteorology Satellite Program (DMSP)	
19. ABSTRACT (Continue on reverse if necessary and identify by block number) Modern military communication, navigation, and surveillance systems depend on reliable, noise-free transionospheric radio-frequency channels. They can be severely impacted by small-scale electron-density irregularities in the ionosphere, which cause both phase and amplitude scintillation. Basic tools used in planning and mitigation schemes are climatological in nature and thus may greatly over- and under-estimate the effects of scintillation in a given scenario. This report summarizes the results of a three-year investigation into the feasibility of using <i>in-situ</i> observations of the ionosphere from the USAF DMSP satellite to calculate estimates of irregularity parameters that could be used to update scintillation models in near real-time. Estimates for the level of intensity and phase scintillation on a transionospheric UHF radio link in the early-evening auroral zone were calculated from DMSP Scintillation Meter (SM) data and compared to the levels actually observed. The intensity scintillation levels predicted and observed compared quite well, but the comparison with the phase scintillation data was complicated by low-frequency phase noise on the UHF radio link. Results are presented from analysis of DMSP SSIES data collected near Kwajalein Island in conjunction with a propagation-effects experiment. Preliminary conclusions to the assessment study are (1) the DMSP SM data can be used to make quantitative estimates of the level of scintillation at auroral latitudes, and (2) it may be possible to use the data as a qualitative indicator of scintillation-activity levels at equatorial latitudes.				
20. DISTRIBUTION/AVAILABILITY OF ABSTRACT <input type="checkbox"/> UNCLASSIFIED/UNLIMITED <input type="checkbox"/> SAME AS RPT. <input type="checkbox"/> DTIC USERS			21. ABSTRACT SECURITY CLASSIFICATION Unclassified	
22a. NAME OF RESPONSIBLE INDIVIDUAL Edward Weber			22b. TELEPHONE (Include Area Code)	22c. OFFICE SYMBOL GL/LIS

TABLE OF CONTENTS

	<u>Page</u>
1. Introduction	1
2. Background	2
3. Analysis of SSIES/AIO/EISCAT Campaign Data	5
4. Summary of Project Results	10
4.1 Study of Methods for Calculation of $C_k L$	10
4.1.1 Procedures for Calculating $C_k L$	10
4.1.2 Uncertainties in $C_k L$	12
4.2 Auroral Region Studies	14
4.3 Equatorial Region Studies	17
5. Conclusion	21
References	23
Appendix. Topside Electron Density Model	25

Accession For	
NTIS GRA&I	<input checked="" type="checkbox"/>
DTIC TAB	<input type="checkbox"/>
Unannounced	<input type="checkbox"/>
Justification	
By	
Distribution /	
Availability Codes	
Dist	
A-1	

LIST OF FIGURES

Figure	Caption	Page
1	Total ion density data from the SSIES Scintillation Meter (SSIES/SM) (a) and the corresponding electron density profiles generated from the SSIES/SM data for the 8 January 1988 pass. The x-axis labels in (a) are for the satellite location, those in (b) are for the 300-km field-line "footprint." The x-axis labels are GLAT for geographic latitude, GLON for geographic longitude, ALT for satellite altitude, APXLAT for modified apex latitude, APXLON for apex longitude, and APXLT for apex local time.	6
2	Data from Figure 1(a) replotted to the "window" sampled by the EISCAT radar. Note the reversal of north and south from Figure 1(a) to this figure.	8
3	Data from the 8 January 1988 campaign day: (a) detrended intensity data from the AIO-AFSAT VHF radio link, (b) detrended phase data from this link, and (c) total ion density from the SSIES/SM sensor. The plots are aligned to cover roughly the same spatial region.	16
4	Comparison of S_4 (a) and σ_ϕ (b) scintillation indices calculated from the AIO-AFSAT intensity and phase data (solid lines) to the corresponding indices calculated from the SSIES C_kL estimates for two irregularity models (17:2 wings plotted as squares, 20:1 rods as diamonds) and those calculated from the WBMOD model (crosses). The two points in (a) labeled "retune" included retune discontinuities, and the point labeled "focus" contained a strong focus. The S_4 values for these points are unreliable.	18
5	Total ion density measured by the SSIES/SM sensor on DMSP F8 near Kwajalein on 24 August 1988. The y-axis is ion density, ranging from 0.0 to 2.0×10^5 ; and the x-axis labels are GMT for Greenwich Mean Time (HH:MM:SS), APXLAT for modified apex latitude, and APXLON for apex longitude.	20

LIST OF TABLES

Table	Caption	Page
1	Parameters for the electron density profiles plotted in Figure 2.	9

PREFACE

This report summarizes the work completed during an investigation into the feasibility of using *in-situ* observations of the ionosphere from the DMSP SSIES sensors to calculate parameters that characterize ionospheric scintillation effects. This work is part of a larger effort with an overall objective of providing the USAF Air Weather Service with the capability of observing ionospheric scintillations, and the plasma density irregularities that cause the scintillations, in near real-time and updating models of ionospheric scintillation with these observations.

1. Introduction

Many modern military systems used for communications, command and control, navigation, and surveillance depend on reliable and relatively noise-free transmission of radiowave signals through the earth's ionosphere. Small-scale irregularities in the ionospheric density can cause severe distortion, known as radiowave scintillation, of both the amplitude and phase of these signals. A basic tool used in estimating these effects on systems is a computer program, WBMOD, based on a single-scatter phase-screen propagation model and a number of empirical models of the global morphology of ionospheric density irregularities^[1,2]. An inherent weakness of WBMOD is that the irregularity models provide median estimates for parameters with large dynamic ranges, which can lead to large under- and over-estimation of the effects of the ionospheric irregularities on a system.

One solution to this problem, at least for near real-time estimates, is to update the WBMOD irregularity models with observations of the various parameters modeled. One proposed source for these observations is from the *in-situ* plasma density monitor to be flown on the Defense Meteorology Satellite Program (DMSP) satellites. Previous studies^[3] using *in-situ* measurements from the DE-2 satellite have found that there is potential for using the data in this fashion. This study is designed to assess the applicability of this data set to real-time updates of the WBMOD models. There are two primary objectives:

- (1) Develop and refine techniques for generating estimates of parameters that characterize ionospheric scintillation from *in-situ* observations of the ionospheric plasma from the DMSP SSIES sensors.
- (2) Determine if the parameters calculated from the SSIES data can be used to compute the scintillation effects on a transionospheric radiowave signal.

This report describes one final aspect of the analysis of data from a campaign conducted near Tromsø in January 1988 and summarizes the findings and results of the entire project.

2. Background

The propagation model used in the WBMOD program (based on weak-scatter phase-screen theory^(1,2)) characterizes the ionospheric electron density irregularities that cause scintillation via eight independent parameters⁽⁴⁾:

- (1) a : The irregularity axial ratio along the direction of the ambient geomagnetic field.
- (2) b : The irregularity axial ratio perpendicular to the direction of the ambient geomagnetic field.
- (3) δ : The angle between sheet-like irregularity structures and geomagnetic L shells.
- (4) h_p : The height of the equivalent phase screen above the earth's surface.
- (5) \underline{v}_d : The *in-situ* irregularity drift velocity.
- (6) α_0 : The outer scale of the irregularity spectrum.
- (7) q : The slope of a power-law distribution that describes the one-dimensional power-density spectrum (PDS) of the irregularities.
- (8) $C_k L$: The height-integrated strength parameter.

The first three parameters (a , b , and δ) and the direction of the ambient geomagnetic field specify the propagation geometry, while the last three (α_0 , q , and $C_k L$) specify the spectral characteristics of the irregularities.

It may be possible to obtain estimates for the values of three of these parameters from the DMSP SSIES sensors: \underline{v}_d (from the SSIES Ion Drift Meter (DM)), and q and $C_k L$ (from the SSIES Ion Scintillation Meter (SM)). In this study, we will focus on the estimation of $C_k L$ from this data set and consider q and \underline{v}_d only in terms of the effects of uncertainties in these parameters on the estimates of $C_k L$. Of the eight parameters, $C_k L$ varies the most as a function of location and time, and has the most profound effect on the accuracy of estimates of scintillation levels made by the WBMOD model.

In the phase-screen propagation theory used in WBMOD⁽⁴⁾, the $C_k L$ parameter is actually the product of two parameters: C_k , the three-dimensional spectral "strength" of the electron density irregularities at a scale size of 1 km^3 (related to the structure constant used in classical turbulence theory); and L , the thickness of the irregularity layer. The models in WBMOD were obtained from analysis of phase scintillation data from the WIDEBAND and HiLat satellites, which will provide estimates of the height-integrated value of $C_k L$ rather than independent

* The cited reference develops the theory in terms of an earlier definition of the strength parameter, C_s , which is defined at a scale size of 2π meters. It is related to C_k according to the equation $C_s = (2\pi/1000)^{4+2} C_k$.

measures of C_k and L . Because of this, the model was developed for $C_k L$ rather than for C_k and L separately.

The calculation of an estimate of the $C_k L$ parameter from topside *in-situ* ion density observations requires two operations. First, an estimate of C_k at the satellite altitude is made from a finite-length time series of density measurements. Second, the estimate of C_k is converted to an estimate of $C_k L$ in some fashion which will account for both the thickness of the irregularity layer and the variation of C_k , or $\langle \Delta N_e^2 \rangle$, within the layer.

The data set from which the estimates of these parameters are to be obtained will be collected by three instruments in the DMSP SSIES (Special Sensor for Ions, Electrons, and Scintillation) sensor package. This data set will contain the following *in-situ* observations:

(1) High time-resolution (24 samples/sec) measurements of the ion density and measurements of the ion density irregularity PDS at high fluctuation frequencies from the Ion Scintillation Meter (SM)^[5].

(2) Measurements of the horizontal and vertical cross-track ion drift velocities from the Ion Drift Meter (DM)^[5].

(3) Measurements of the ion and electron temperatures, the densities of O^+ and the dominant light ion (H^+ or He^+), and the horizontal ram ion drift velocity from the ion Retarding Potential Analyzer (RPA)^[6].

The basic data of this set are the high time-resolution density data from the SM which will be used to generate estimates of the irregularity PDS. The drift-velocity measurements from the DM and RPA will be used in calculating an estimate of C_k from parameters obtained from the PDS, and the other measurements from the RPA will be used in calculating $C_k L$ from C_k .

In the first year of this project, techniques for calculating estimates of $C_k L$ from the SSIES data set were developed, and parametric studies were conducted to determine the uncertainties in the final $C_k L$ estimates due to uncertainties in the parameters and procedures used to calculate the estimates. Since the first SSIES sensor package was not flown until mid-1987, these studies were conducted using simulated SM density data sets and phase scintillation data from the Wideband satellite. The results of these studies were reported in Scientific Report 1 for this project^[7] (herein referred to as Report 1) and will be summarized in Section 4.1 of this report.

The second phase of the project, which focuses on how well these techniques work using data from the DMSP F8 and F9 spacecraft, was begun during the second year of the project. A coordinated, multi-sensor observation campaign was conducted during January 1988 in the vicinity of Tromsø, Norway, in order to collect data for this study. The GL Airborne Ionospheric Observatory (AIO) aircraft flew repeated north-south legs along the magnetic meridian at times when the DMSP F8 satellite was passing overhead. Data collected on the AIO included

intensity and phase scintillation observations on a VHF link from an AFSAT satellite, auroral images from an all-sky photometer, and ionograms from a digisonde. Ionospheric soundings by the EISCAT incoherent-scatter radar located in Norway also were made aperiodically throughout the observation period. Data were collected for DMSP passes on 8, 9, 15, 16, 17, and 18 January 1988. The procedures used to process these data and results from the analysis were reported in Scientific Reports 2 and 3 for this project^[8,9] (herein referred to as Reports 2 and 3) and will be summarized in Section 4.2.

During the third year, a complete analysis was made SSIES data collected from both DMSP F8 and F9 during a multi-sensor campaign conducted by the Defense Nuclear Agency (DNA) near Kwajalein Island were analyzed to determine the usefulness of these data for scintillation characterization in the equatorial ionosphere. The results of these studies were presented in Report 3 and are summarized in Section 4.3 of this report.

A note on coordinate systems: The geomagnetic latitude, longitude, and local time coordinate system used throughout this report is modified apex coordinates^[10], a coordinate system derived from apex coordinates proposed by VanZandt *et al*^[11]. This system, which is used in the WBMOD model, was chosen because it is very similar to both invariant and corrected geomagnetic coordinates at high latitudes, and modified apex latitude is very similar to dip latitude in the equatorial region, becoming identical to dip latitude at the dip equator.

3. Analysis of SSIES/AIO/EISCAT Campaign Data

In Report 3, the results from a detailed analysis of the data collected on 8 January 1988 were presented. One aspect of the data analysis which was not presented in detail was a discussion of the electron density profiles used to generate the effective layer thickness parameter, L_{eff} , which is used in turn to calculate an estimate of $C_k L$ from the C_k value derived from the *in-situ* Scintillation Meter (SM) ion density measurements. In this section we will describe the way in which these profiles were generated and present examples of the profiles used in the 8 January analysis.

The model used to generate the profiles is a two-component diffusive-equilibrium model developed several years ago for building profiles from SSIES observations (see Appendix). Inputs to the model include the critical frequency of the F2 peak and the height of the peak (f_oF2 and h_mF2), the semi-thickness of the topside just above the F2 peak, the electron density (or total ion density) at some height in the topside, and either the height at which the O+ and H+ number densities are equal (i.e., the O+/H+ transition height) or the ratio of O+ to H+ at some height in the topside. In addition, the model has several "free" parameters which can be adjusted to change the shape of the profile. Any of the input parameters can be adjusted within the model to fit the profile to the other inputs. For example, in the present study the f_oF2 and h_mF2 values were adjusted to fit the profile to the total ion density observed by the SM sensor.

The procedures to build the profile used to calculate L_{eff} were as follows:

- (1) Calculate the average total ion density for the data set used to calculate C_k from the density-trend time series removed from the SM density measurements in the detrending process.
- (2) Trace down the field line passing through the center of the data sample to an altitude of 300 km.
- (3) Calculate estimates of f_oF2 and h_mF2 using the CCIR coefficients for f_oF2 and M3000 and values for the O+/H+ transition height and the topside semi-thickness at this location.
- (4) Iteratively adjust the f_oF2 and h_mF2 parameters to fit the profile to the average density calculated in step (1).

This profile and a model for the height variation of the irregularity strength as a function of the background plasma density are then used to calculate L_{eff} .

Figure 1 shows the SM density record from the 8 January 1988 pass near Tromsø (upper plot) and a contour plot of the corresponding electron density profiles which were generated to calculate L_{eff} . The locations and geomagnetic local time (APXLT) along the x-axis of the *in-situ* density plot are calculated at the satellite altitude, and those along the x-axis of the profile plot are calculated at the 300km "footprint" of the field line passing through the satellite location.

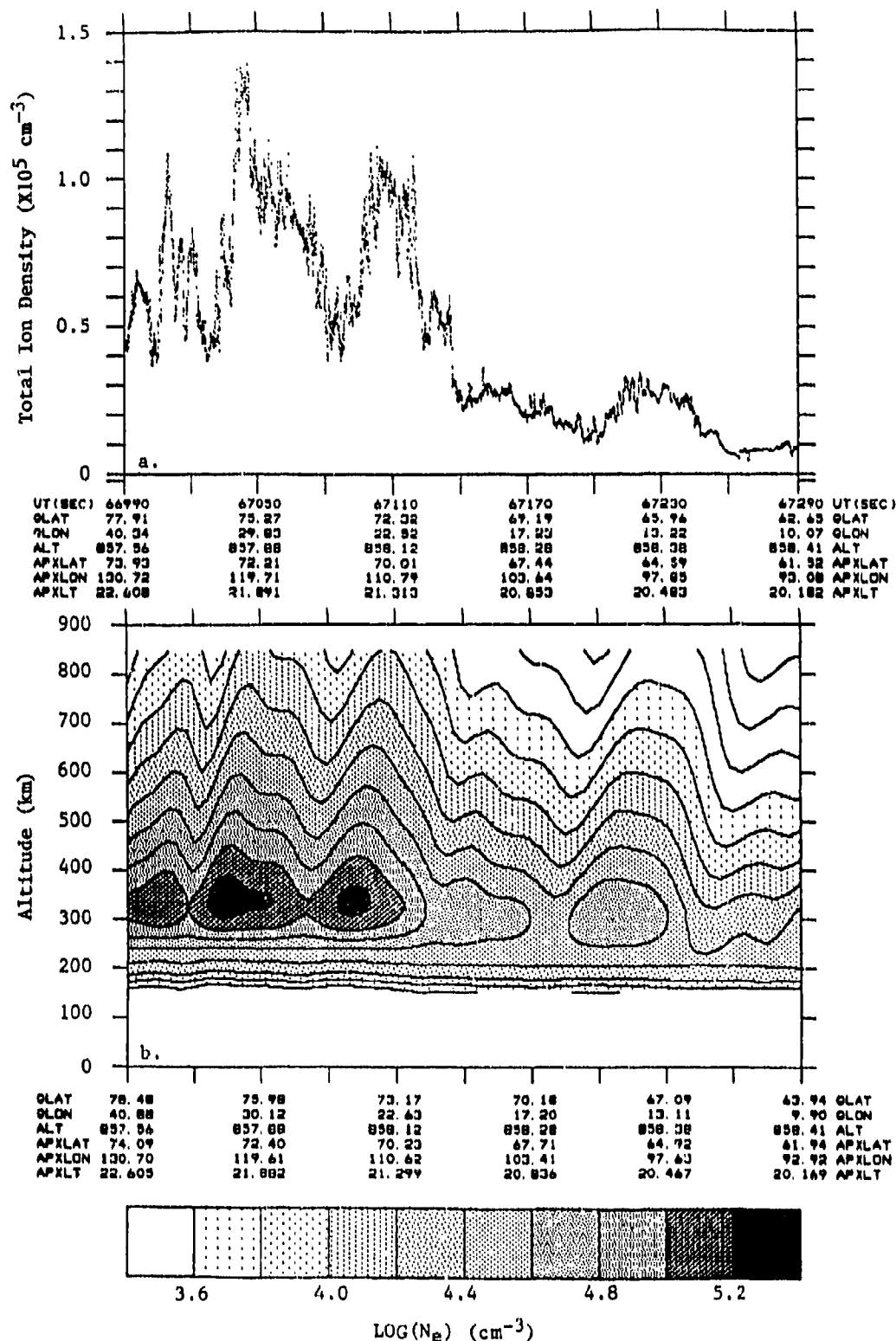


Figure 1. Total ion density data from the SSIES Scintillation Meter (SSIES/SM) (a) and the corresponding electron density profiles generated from the SSIES/SM data for the 8 January 1988 pass. The x-axis labels in (a) are for the satellite location, those in (b) are for the 300-km field-line "footprint." The x-axis labels are GLAT for geographic latitude, GLON for geographic longitude, ALT for satellite altitude, APXLAT for modified apex latitude, APXLON for apex longitude, and APXLT for apex local time.

The slight tilt to the right in the profile plot is due to mapping the profiles constructed along field lines. [Note: The profile plot shows no ionization in the E region because the model used does not include an auroral precipitation-produced E region, and there is no solar component as the E region is dark throughout the pass. This does not affect the results, however, as the model used to calculate C_kL assumes that all contributions to the integrated irregularity strength come from the F2 region.]

Our initial hope was to use profiles from the EISCAT radar as part of the study, but there have been difficulties in putting the radar data into useful form. One figure showing a contour plot of electron density from a roughly north-south meridional scan from the radar with a center time of 18:34:40 GMT (66800 seconds past midnight) has been received for comparison with the profiles used in the L_{eff} calculation. Unfortunately, this figure is in color and could not be legibly reproduced in black and white for this document.

We have, however, replotted a subset of the model profiles in the same format as the color figure showing what the radar would have seen if it had sampled our model ionosphere (Figure 2). This figure has the same contour levels as in Figure 1, but the x-axis has been reversed (north is now to the right) and is plotted in the corrected geomagnetic (CG) latitude of the 300 km "footprint" location. The irregular shape of the sampled region corresponds to that shown in the color plot provided of the EISCAT data. The model parameters used to build these profiles and the resulting L_{eff} values are listed in Table 1.

Quantitatively, the radar data and model "prediction" agree fairly well. Both show an F2-region enhancement at the northern edge of the sampled region, a lesser enhancement at the southern edge, a "tongue" of enhanced density reaching from the northern enhancement to the center of the sampled region, and a region of low plasma in the topside between CG latitude 65.5° and 68° . There are some discrepancies in details. The altitudes of the peak in the model profiles average about 30-50 km above the estimated peaks in the radar data, and the enhancement at the northern end of the region is further from Tromsø in the radar data than is shown in the model profiles. Unfortunately, no quantitative comparison of the density levels was possible as the color plot of the radar data was of relative rather than absolute density.

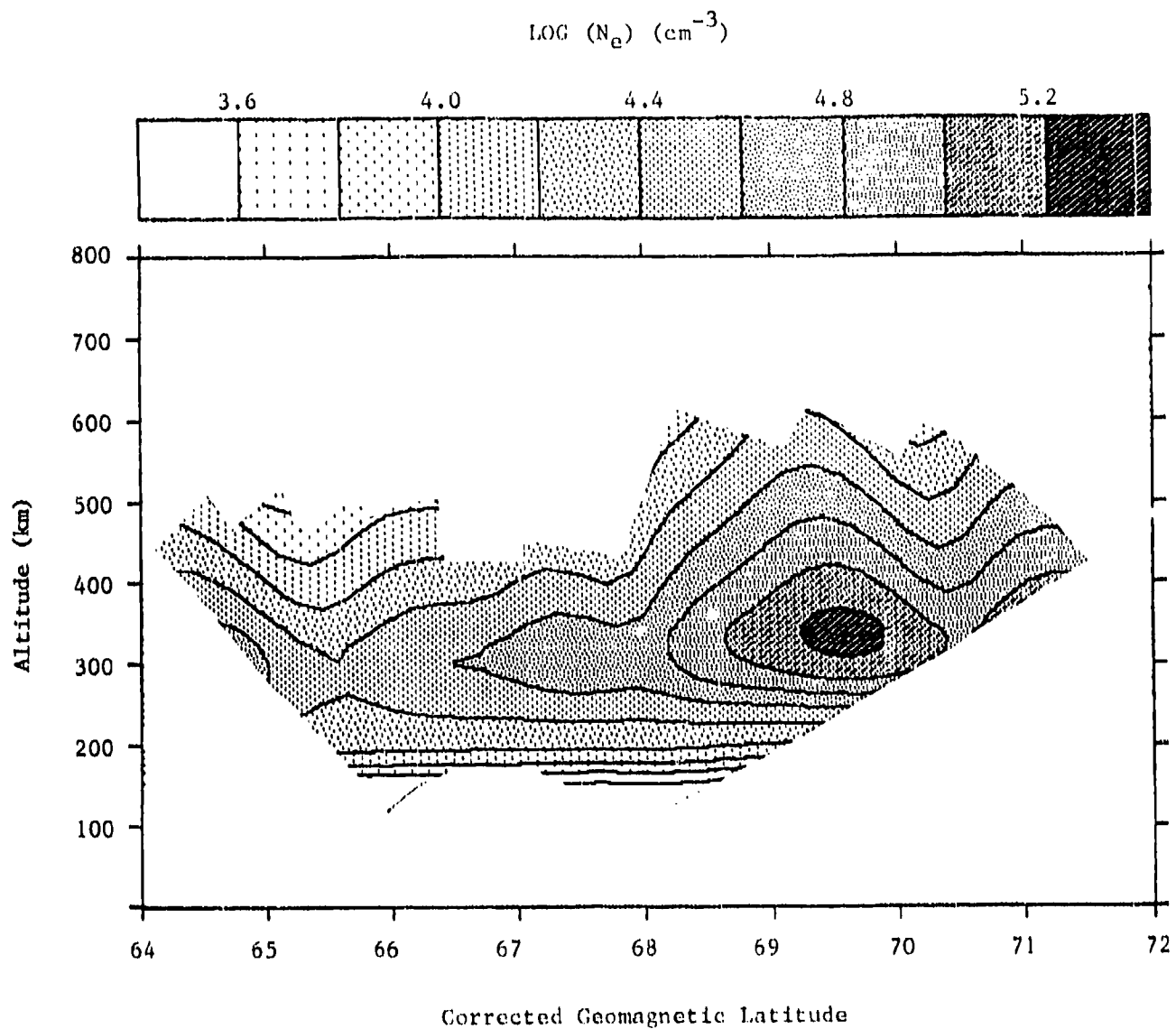


Figure 2. Data from Figure 1(a) replotted to the "window" sampled by the EISCAT radar. Note the reversal of north and south from Figure 1(a) to this figure.

TIME	GLAT	GLON	CGLAT	CGLON	FoF2z	foF2	hmf2z	hmf2	Yt	Ht	I	Loft
67055	75.76	29.39	71.61	118.88	2.85	3.87	327.95	344.71	84.274	1195.13	3	3.151E+07
67060	75.53	28.68	71.43	118.10	2.82	3.68	327.62	342.08	83.887	1195.13	3	3.266E+07
67065	75.30	27.99	71.26	117.32	2.80	3.64	327.28	341.35	83.508	1195.13	3	3.289E+07
67070	75.07	27.33	71.08	116.56	2.77	3.64	326.95	341.13	83.142	1195.13	3	3.287E+07
67075	74.84	26.68	70.90	115.81	2.75	3.52	326.61	339.37	82.786	1195.13	3	3.362E+07
67080	74.61	26.05	70.72	115.06	2.73	3.27	326.27	335.44	82.440	1195.13	2	3.549E+07
67085	74.37	25.44	70.53	114.31	2.70	2.97	325.93	330.61	82.105	1195.13	2	3.797E+07
67090	74.13	24.85	70.33	113.57	2.68	2.85	325.59	328.58	81.779	1195.13	2	3.897E+07
67095	73.90	24.27	70.15	112.88	2.66	3.03	325.25	331.50	81.463	1195.13	2	3.713E+07
67100	73.66	23.70	69.96	112.20	2.64	3.38	324.90	336.70	81.158	1195.13	2	3.424E+07
67105	73.42	23.16	69.76	111.54	2.61	3.69	324.55	339.86	80.861	1195.13	3	3.255E+07
67110	73.17	22.63	69.55	110.88	2.59	3.81	324.21	340.60	80.575	1195.13	3	3.207E+07
67115	72.93	22.11	69.36	110.23	2.57	3.72	323.86	339.52	80.297	1195.13	3	3.245E+07
67120	72.68	21.60	69.15	109.57	2.55	3.49	323.51	336.94	80.028	1195.13	3	3.355E+07
67125	72.44	21.11	68.95	108.93	2.53	3.22	323.16	333.57	79.769	1195.13	2	3.510E+07
67130	72.19	20.63	68.74	108.29	2.51	3.00	322.81	330.30	79.518	1195.13	2	3.666E+07
67135	71.94	20.17	68.53	107.66	2.49	2.79	322.45	327.06	79.281	1195.13	2	3.829E+07
67140	71.69	19.71	68.31	107.08	2.48	2.50	322.10	322.49	79.064	1195.13	1	4.079E+07
67145	71.45	19.27	68.11	106.53	2.46	2.20	321.75	317.74	78.855	1195.13	2	4.360E+07
67150	71.19	18.83	67.88	105.95	2.44	2.09	321.39	316.10	78.652	1195.13	2	4.449E+07
67155	70.94	18.41	67.67	105.39	2.43	2.18	321.04	317.27	78.457	1195.13	2	4.354E+07
67160	70.69	18.00	67.45	104.84	2.41	2.22	320.68	317.85	78.269	1195.13	2	4.300E+07
67165	70.44	17.60	67.23	104.30	2.40	2.14	320.32	316.46	78.087	1195.13	2	4.373E+07
67170	70.18	17.20	67.00	103.74	2.38	2.01	319.97	314.44	77.913	1195.13	2	4.492E+07
67175	69.93	16.82	66.78	103.22	2.37	1.95	319.61	313.45	77.745	1195.13	2	4.543E+07
67180	69.67	16.44	66.55	102.71	2.36	1.94	319.26	313.18	77.584	1195.13	2	4.546E+07
67185	69.42	16.08	66.33	102.23	2.34	1.90	318.90	312.42	77.430	1195.13	2	4.584E+07
67190	69.16	15.72	66.10	101.74	2.33	1.79	318.54	310.87	77.283	1195.13	2	4.678E+07
67195	68.90	15.37	65.87	101.26	2.32	1.66	318.19	308.99	77.142	1195.13	3	4.801E+07
67200	68.65	15.03	65.65	100.79	2.31	1.58	317.83	307.76	77.008	1195.13	3	4.880E+07
67205	68.39	14.69	65.41	100.31	2.30	1.64	317.47	308.31	76.881	1195.13	3	4.825E+07
67210	68.13	14.36	65.18	99.84	2.29	1.85	317.12	310.88	76.760	1195.12	2	4.624E+07
67215	67.87	14.04	64.94	99.38	2.29	2.08	316.76	313.84	76.646	1195.12	2	4.411E+07
67220	67.61	13.72	64.70	98.94	2.28	2.21	316.41	315.49	76.538	1195.12	1	4.294E+07
67225	67.35	13.41	64.46	98.49	2.27	2.23	316.05	315.48	76.437	1195.18	1	4.286E+07
67230	67.09	13.11	64.21	98.06	2.27	2.20	315.70	314.75	76.342	1195.26	1	4.324E+07
67235	66.83	12.82	63.96	97.63	2.26	2.17	315.35	314.04	76.253	1195.31	1	4.362E+07

Legend:

TIME	Seconds since midnight (GMT)
GLAT	Geographic latitude
GLON	Geographic longitude
CGLAT	Corrected Geomagnetic latitude
CGLON	Corrected Geomagnetic longitude
foF2z	Initial foF2 (from CCIR)
foF2	foF2 from profile fit to in-situ density
hmf2z	Initial hmf2 (from CCIR)
hmf2	hmf2 from profile fit to in-situ density
Yt	Topside layer thickness parameter
Ht	O+/H+ transition height
N	Number of iterations for profile fit
Loft	Effective layer thickness parameter (m)

[Note: All locations have been traced down the local field line to 300 km altitude.]

Table 1. Parameters for the electron density profiles plotted in Figure 2.

4. Summary of Project Results

4.1 Study of Methods for Calculation of $C_k L$

The goal of this study was to develop a method for calculating an estimate of $C_k L$ from data collected by the SSIES plasma probes and to make a determination of the uncertainties in these estimates.

4.1.1 Procedures for Calculating $C_k L$

According to phase-screen theory^[2], if the power-density spectrum (PDS) of the plasma density irregularities are assumed to follow a single-regime power-law model, an estimate for the spectral strength parameter, C_k , can be calculated from *in-situ* measurements of the plasma density irregularities from

$$C_k = 5.0 \times 10^8 \, q \left(\frac{10^3}{v_p} \right)^{q-1} T_1 \quad [1]$$

where q and T_1 are the slope and intercept of a log-linear fit to the PDS calculated from the plasma density data, and v_p is an effective velocity of the satellite with respect to the irregularities. This last parameter is defined in a coordinate system defined by the geometry of the irregularities and is given by

$$v_p = \underline{v}^T \underline{C} \underline{v} \quad [2]$$

where \underline{v} is the vector velocity of the satellite with respect to the irregularities (which includes the satellite's orbital velocity and the *in-situ* velocity of the irregularities), and \underline{C} is a transformation matrix derived from a generalized model of the irregularity geometry^[12].

The procedure developed for calculating parameters q and T_1 from the SSIES Scintillation Meter ion density data is as follows:

- (1) Detrend the ion density data by removing a background trend. This trend can be calculated from either a low-pass filter applied to the entire data set or a quadratic least-squares fit to each data sample (256 or 512 points).
- (2) Apply a time-domain window to the detrended data sample. The window of choice is a 30% split-bell cosine taper.
- (3) Use an FFT of the detrended, windowed data sample to calculate an estimate of the PDS ($\Phi_{\Delta N}$).

- (4) Smooth the PDS estimate. The smoothing function used is a five-point, centered function with binomial weights.
- (5) Use a linear least-squares fit to $\log(\text{PDS})$ versus $\log(\text{frequency})$ over the frequency range 0.3 to 5.0 Hz.

The various parameters in this method, such as the severity of the windowing function and the frequency range for the PDS fit, were determined from a series of parametric studies using simulation data generated with known spectral characteristics (see Report 1) and were validated against a sample of data from the SM sensor on DMSP satellite F8 (see Report 2).

The calculation of and estimate of $C_k L$ from an observation of C_k at the satellite altitude, h_s , is based on the following assumptions:

- (1) The altitude at which the C_k measurement is made is within the irregularity layer.
- (2) The measured C_k is representative of conditions throughout the irregularity layer.
- (3) The geometry of the irregularities, and the slope of the irregularity PDS, are relatively constant throughout the height range of the irregularity layer.
- (4) The variation of C_k , or $\langle \Delta N^2 \rangle$, with altitude throughout the irregularity layer is known, or can be modeled.

These assumptions lead the following relationship between $C_k L$ and C_k :

$$C_k L = C_k L_{\text{eff}} \quad [3]$$

where L_{eff} is an effective layer thickness parameter, given by

$$L_{\text{eff}} = \frac{\int_{h_b}^{h_s} \langle \Delta N^2 \rangle dh}{\langle \Delta N^2 \rangle_s} \quad [4]$$

where h_b is the height of the bottom of the irregularity layer and $\langle \Delta N^2 \rangle_s$ is the density variance at the satellite altitude.

For this project, we have chosen a simple model for the variation of $\langle \Delta N^2 \rangle$ with altitude which assumes that the layer extends from 1/4 of a scale height below the F2-layer peak height

to the satellite altitude, and that the ratio of $\langle \Delta N^2 \rangle$ to the background density is constant throughout the layer. This changes Equation [4] to

$$L_{eff} = \frac{\int_{h_b}^{h_s} N_e^2(h) dh}{N_e^2(h_s)} \quad [5]$$

where $N_e(h)$ is the height variation of the electron density. We have used a two-component (O+ and H+) model of the topside ionosphere developed specifically for use with the SSIES data set for $N_e(h)$ [13]. The application of this model to the problem at hand was described in Section 3.

In summary, estimates of $C_k L$ were calculated from the SSIES SM sensor data using the following steps:

- (1) Calculate q and T_1 from the SM ion density data records using either 256- or 512-point data samples.
- (2) Calculate the effective velocity, v_p , from the satellite orbital velocity, observations or model values for the *in-situ* drift velocity of the irregularities, and models for the irregularity geometry taken from the WBMOD scintillation model [2].
- (3) Calculate C_k using Equation [1].
- (4) Fit the $N_e(h)$ model to the average plasma density of the data sample by adjusting the F2 peak density and height parameters (see Section 3).
- (5) Calculate L_{eff} using the fitted model and Equation [5].
- (6) Calculate $C_k L$ using Equation [3].

4.1.2 Uncertainties in $C_k L$

The effects of uncertainties in various parameters used in the calculation of $C_k L$ on the final $C_k L$ were investigated and quantified (see Sections 3 and 4 in Report 1). Three sources of uncertainty studied were errors in the values of q and T_1 , errors in v_p , and errors in L_{eff} .

The errors inherent in the calculation of q and T_1 from a plasma density sample were estimated using a set of 192 simulated data samples generated with known spectral characteristics, including values for q varying across the nominal expected range of this parameter (1.0 to 3.0) (see Appendix A of Report 1 for the details of this simulated data set). The RMS error in

estimating α and T_1 from this data set using the procedures outlined earlier were 3.3% and 6.7%, respectively. The resulting uncertainty in C_k (and, ultimately, in $C_k L$) due to these RMS "error bars" is a function of the effective velocity (v_p), ranging from 6 to 11% for values of v_p of 1000 to 7000 m/s. The average uncertainty due to this source should be on the order of 8-10%.

The effective velocity is a function of the satellite velocity (v_s), the *in-situ* drift velocity of the irregularities (v_d), and the irregularity geometry which includes the orientation of the irregularities and their axial ratios (a and b). The velocity of the satellite due to its orbital motion is fairly well determined, as is the orientation of the irregularities (determined to first order by the local geomagnetic field direction), so the major sources of uncertainty in this parameter are in the *in-situ* drift velocity and the axial ratios of the irregularities. In order to reduce the complexity of the problem, the parametric studies conducted were limited to the geometries expected for a satellite in a nominal DMSP orbit.

The effects of uncertainties in these parameters on $C_k L$ are fairly complex, but can be summarized as follows:

- (1) Uncertainties in axial ratio a had a minimal effect on $C_k L$. A $\pm 50\%$ uncertainty in a results in less than a 2% uncertainty in $C_k L$ at high latitudes, and rarely in more than 5% at other latitudes.
- (2) Uncertainties in axial ratio b , which specifies how elongated the irregularities are across the geomagnetic field, had a much larger effect at high latitudes (there is no effect at other latitudes, as sheet-like irregularities occur only in the auroral region). A $\pm 50\%$ uncertainty in b can result in a 25-100% uncertainty in $C_k L$.
- (3) If measurements of the *in-situ* drift velocity are available from the SSIES Drift Meter and Retarding Potential Analyzer, the expected uncertainties in these observations will lead to 5-10% uncertainties in $C_k L$. If these measurements are not available, the average uncertainty in $C_k L$ increases to 10-20% and may be as high as 30-40%.

As a function of location, the uncertainties in $C_k L$ due to uncertainties in v_p in the equatorial region should be on the order of 5 to 10% when the *in-situ* drift velocities are known and 10 to 20% when they are not; in the auroral region they should be 5 to 10% when v_d and b are known, 15 to 30% when v_d is not well known (i.e., not observed), and 25 to >100% when neither are well known.

The effects of uncertainties in L_{eff} on $C_k L$ were studied by varying parameters of the density profile model around values nominal for regions which will be sampled by the DMSP satellites. The results of this study were as follows:

- (1) The most crucial profile parameter for making accurate estimates of $C_k L$ is the plasma density at the F2 peak. An error of 20% in $f_o F2$ can result in errors of 100% in $C_k L$.
- (2) The effects of errors in the density at the satellite can be as serious as those due to errors in $f_o F2$, but this parameter will be measured routinely with an accuracy of about $\pm 5\%$, which results in a $\pm 8-10\%$ uncertainty in $C_k L$.
- (3) The uncertainty in $C_k L$ is much more sensitive to errors in the ratio of the density at the satellite to the peak density than to absolute (correlated) errors in the two values. It is important that the two densities be consistent with one another.
- (4) The effects of 20% errors in the other profile parameters, most of which describe the shape of the profile, resulted in less than 10% errors in $C_k L$.

4.2 Auroral Region Studies

In order to assess the limitations of using $C_k L$ calculated from the DMSP SSIES data to characterize transionospheric scintillation in the auroral zone, a data-collection campaign was conducted in the vicinity of the EISCAT incoherent radar facility at Tromso, Norway, during January 1988. The primary objective of the SSIES/AIO/EISCAT campaign was to make near-coincident observations of the state of the ionosphere and of a radio signal propagating through the ionosphere in order to assess the validity of using information from the SSIES SM sensor to characterize and quantize the effects of scintillation on a transionospheric radio transmission. The concept was to use estimates of the scintillation parameters $C_k L$ and q derived from the SSIES SM density data to calculate estimates of the level of phase and amplitude scintillation to be expected on a specific transionospheric satellite communications link, and then to compare these to the scintillation levels actually observed on that link.

The following data were collected during this campaign:

- (1) From the DMSP F8 satellite:
 - (a) *In-situ* observations of the total ion density (N_i) at a data rate of 24 samples/sec from the SSIES SM sensor.
 - (b) *In-situ* observations of the horizontal (u_h) and vertical (u_v) cross-track components of the ion drift velocity at a data rate of 6 samples/sec from the SSIES DM (Drift Meter) sensor.
 - (c) *In-situ* observations of precipitating electrons and ions at a data rate of one energy spectrum per second from the SSJ/4 sensor.

(2) From the AFGL Airborne Ionospheric Observatory (AIO):

- (a) Phase and amplitude records of a 250MHz radio transmission from an AFSAT satellite (#7225).
- (b) All-sky photometer images at three wavelengths (4278A, 5577A, and 6300A) at a data rate of (at least) one image per wavelength per minute from the All-Sky Imaging Photometer (ASIP).
- (c) Ionospheric soundings at a data-rate of approximately one sounding every two to three minutes from the Digisonde.

(3) From the EISCAT incoherent radar:

- (a) Electron density profiles along a near-meridian-plane scan.
- (b) Electron and ion temperature profiles along a near-meridian-plane scan.
- (c) Ion drift velocity profiles along a near-meridian-plane scan.

[Note: We had hoped to process data from the SSIES Retarding Potential Analyzer (RPA) sensor to obtain observations of the ion temperature and the ratio of the number density of O⁺ ions to H⁺ (or He⁺) ions, both of which would have been used in the calculation of $C_k L$. Unfortunately, this instrument failed prior to the first campaign period.]

One data set was collected during each day of the campaign (8-9 and 15-18 January 1988). The DMSP F8 satellite is in a nominal dawn-dusk orbit which, during the two campaign collection intervals, passed the satellite near the EISCAT facility at around 1830UT. The observing plan was to have the AIO fly a north-south pattern configured so that the ionospheric penetration point of the AIO-AFSAT radio link passed near the DMSP orbit track, and for the EISCAT facility to conduct north-south meridian scans roughly aligned with the DMSP track at the time of the overpass. Estimates of $C_k L$ were calculated for each of the six passes, and the results were catalogued in Appendix A of Report 2. Due to limited resources and time, the analysis focused on the data collected on 8 January 1988. The details of this analysis can be found in Section 3 of Report 3.

Figure 3 summarizes the basic data used in the analysis. Plots (a) and (b) in this figure are the intensity and phase data, respectively, from the AIO-AFSAT VHF beacon link, and Plot (c) is the Scintillation Meter (SM) density data from DMSP satellite F8. The time interval of the SM data plot was chosen so that the geomagnetic latitudes covered by this plot is identical to that covered by the AIO-AFSAT plots. Estimates for $C_k L$ and q were generated from the SM data which were then used to calculate the scintillation parameters S_4 and σ_ϕ using the phase-screen propagation model in the WBMOD scintillation code^{11,41} and two models for the irregularity axial ratios (20:1 rods and 17:2 wings). The same parameters were calculated (in the time domain) from the AIO-AFSAT intensity and phase data, respectively.

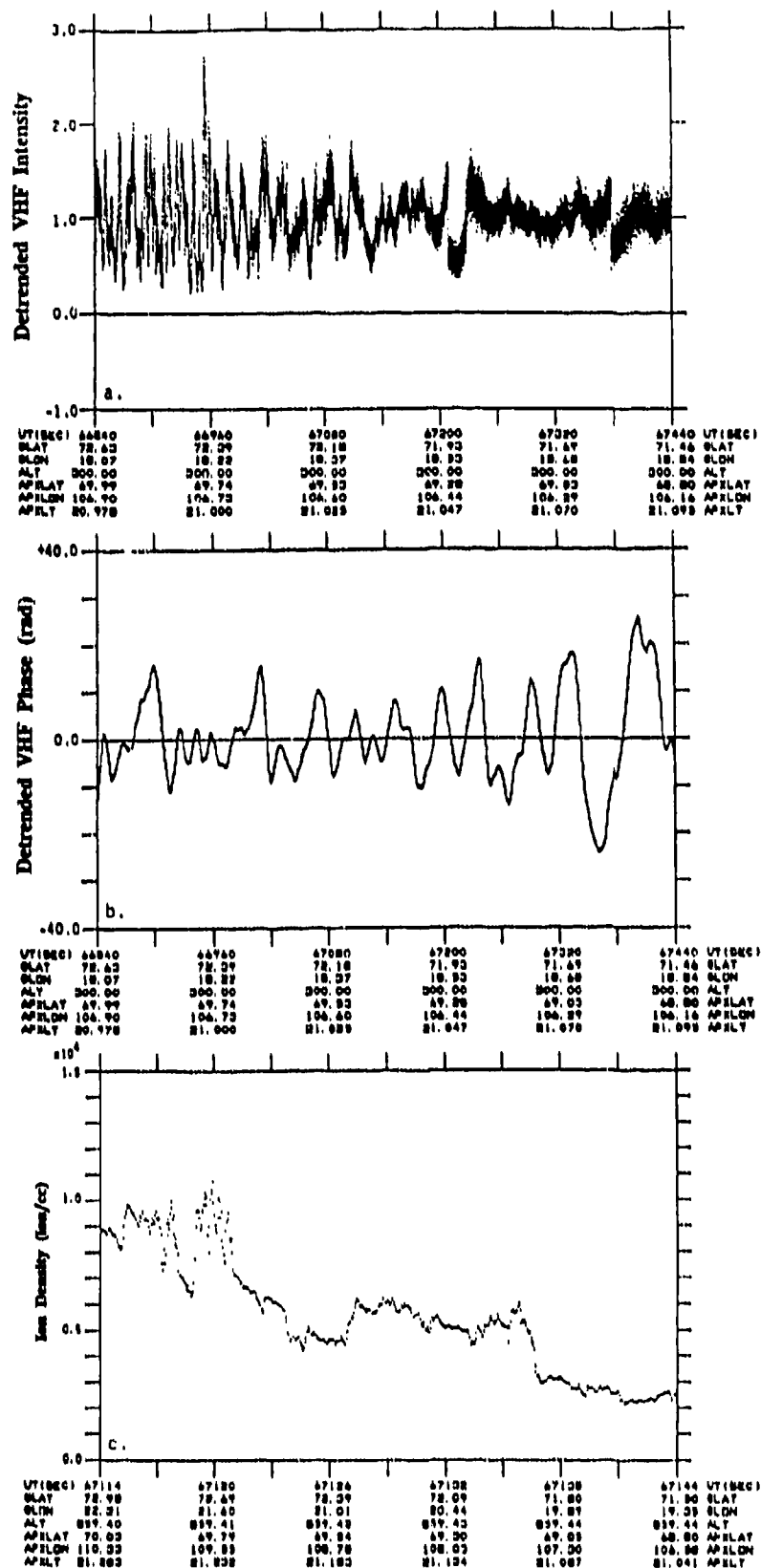


Figure 3. Data from the 8 January 1988 campaign day: (a) detrended intensity data from the AIO-AFSAT VHF radio link, (b) detrended phase data from this link, and (c) total ion density from the SSIES/SM sensor. The plots are aligned to cover roughly the same spatial region.

Figure 4 shows the results of these calculations. The solid lines in these figures are the indices calculated from the beacon data in Figure 3, and the diamonds and squares are values calculated from the SM C_kL and q values. The crosses indicate values generated by the WBMOD models for C_kL and q . The agreement between the S_4 values generated from the DMSP data and that calculated from the beacon data is quite good, particularly in light of the many assumptions which went into the C_kL calculation. The agreement between the σ_ϕ values is almost as bad as the agreement between the S_4 values was good. The validity of the phase data has been called into question, however, by the presence of unexplained high levels of low-frequency power in the phase data which does not appear to be correlated with anything geophysical. Attempts were made to remove this low-frequency power by detrending and by comparing the phase and *in-situ* power-density spectra, but no clear, supportable results were obtained.

The final conclusion of this study was that the excellent agreement between the S_4 values predicted by the SM density data and those observed on the AIO-AFSAT radio link indicate that there is potential for using the SM data in the auroral region for characterizing transionospheric scintillation levels. This assessment should be confirmed, however, by a similar analysis of data collected during a second campaign in the Tromsø area during January 1990. In this second campaign, AFSAT beacon data were collected both on the AIO aircraft and on a ground receiver near Tromsø^[14].

4.3 Equatorial Region Studies

During the month of August, 1988, the Defense Nuclear Agency (DNA) conducted an extensive multi-sensor data-collection campaign near Kwajalein Island to assess the effects of ionospheric scintillation on radar signal propagation (Propagation Effects Assessment - Kwajalein, or PEAK). This campaign was used as a target of opportunity to conduct an assessment of the potential for using the DMSP SSIES data for characterizing scintillation in the equatorial region. The purpose of the DNA PEAK campaign was to collect data from a number of ionospheric probes, both remote and *in-situ*, which could be used to characterize plasma density irregularities in the equatorial ionosphere in order to assess the effect of these irregularities on transionospheric radar propagation. The campaign ran during the period 3-31 August 1988, with most of the ground-based instruments located on islands in the Kwajalein Atoll (9°24'N, 167°28'E). Of the various data sets collected, the following have been made available for this study:

- a. SSIES data from both F8 and F9 DMSP satellites for the entire month of August.
- b. Intensity scintillation data (S_4) from a UHF link from Kwajalein Island to a FLTSAT satellite located over the equator at 172° E longitude for the period 3-31 August.

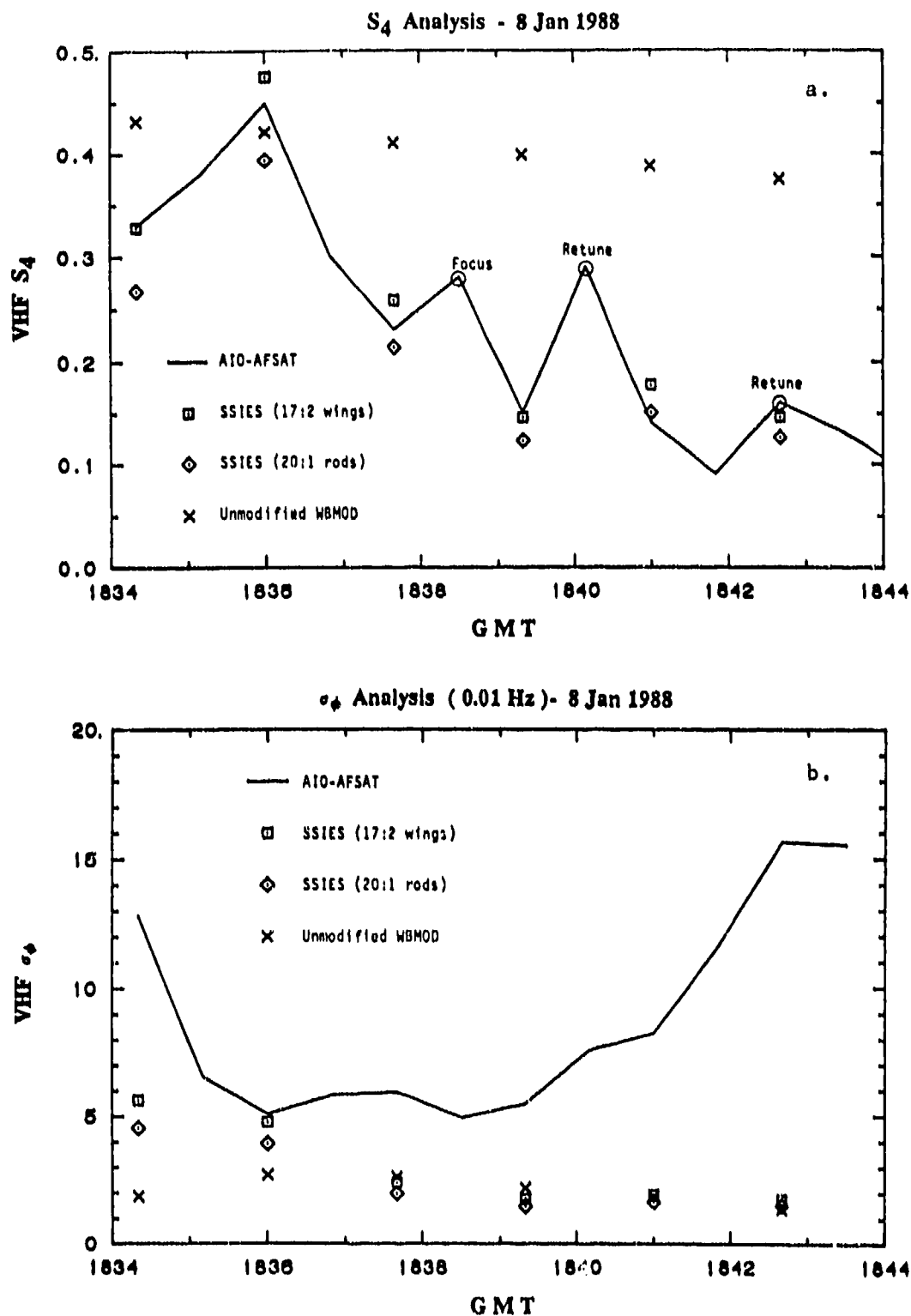


Figure 4. Comparison of S_4 (a) and σ_ϕ (b) scintillation indices calculated from the AIO-AFSAT intensity and phase data (solid lines) to the corresponding indices calculated from the SSIES $C_k L$ estimates for two irregularity models (17:2 wings plotted as squares, 20:1 rods as diamonds) and those calculated from the WBMOD model (crosses). The two points in (a) labeled "retune" included retune discontinuities, and the point labeled "focus" contained a strong focus. The S_4 values for these points are unreliable.

c. Intensity scintillation data (S_4) from UHF and L-band links to the HiLat and Polar BEAR satellites obtained at Kwajalein Island with the DNA ROVER receiver for the period 1-29 August.

In this study, attempts were made to correlate observations of plume structures in the SSIES DM density data (such as that shown in Figure 5) with the FLTSAT and HiLat/Polar BEAR scintillation observations, and to corroborate a threshold effect observed in DMSP Retarding Potential Analyzer data in an earlier study^[15] (this will be denoted the RPA Study). Details of the study can be found in Section 4 of Report 3.

The results of this study were consistent with and, for the most part, confirmed those reported in the RPA Study. The main results were as follows:

- (1) Due to the inclination of the DMSP orbit, the orientation of the equatorial plume structures with the local geomagnetic meridian, and, possibly, the altitude of the DMSP orbit, there is a significant probability that the satellite may pass through an equatorial region populated by plume structures and not intersect one. There were several cases in the study period where S_4 on the FLTSAT link was saturated for most of the evening yet there were no plume-structure signatures in the DMSP data.
- (2) If a plume-structure signature is found in the DMSP data, radio links in the same longitude sector will experience periods of severe scintillation.
- (3) There may be a threshold effect in the background density observations which might be used to infer the presence of plume structures even though none were encountered directly by the satellite. Similar effects were seen in both studies, but the threshold levels found differed by as much as a factor of 2, and there may be an unacceptably high false-alarm rate.

The conclusion of this study was that the DMSP data would be of limited use for making direct observations of plume structures in the equatorial night region, but that the data might be used in indirect ways to infer the probability of the presence of these structures. A more detailed study using a multi-year database of DMSP density data and any available equatorial scintillation data should be conducted to develop and test such indirect methods. If there is a density-threshold effect, the results of an expanded study might also provide a basis for using the output of improved models of the background plasma density as an input to the equatorial C_kL model in the WBMOD scintillation model.

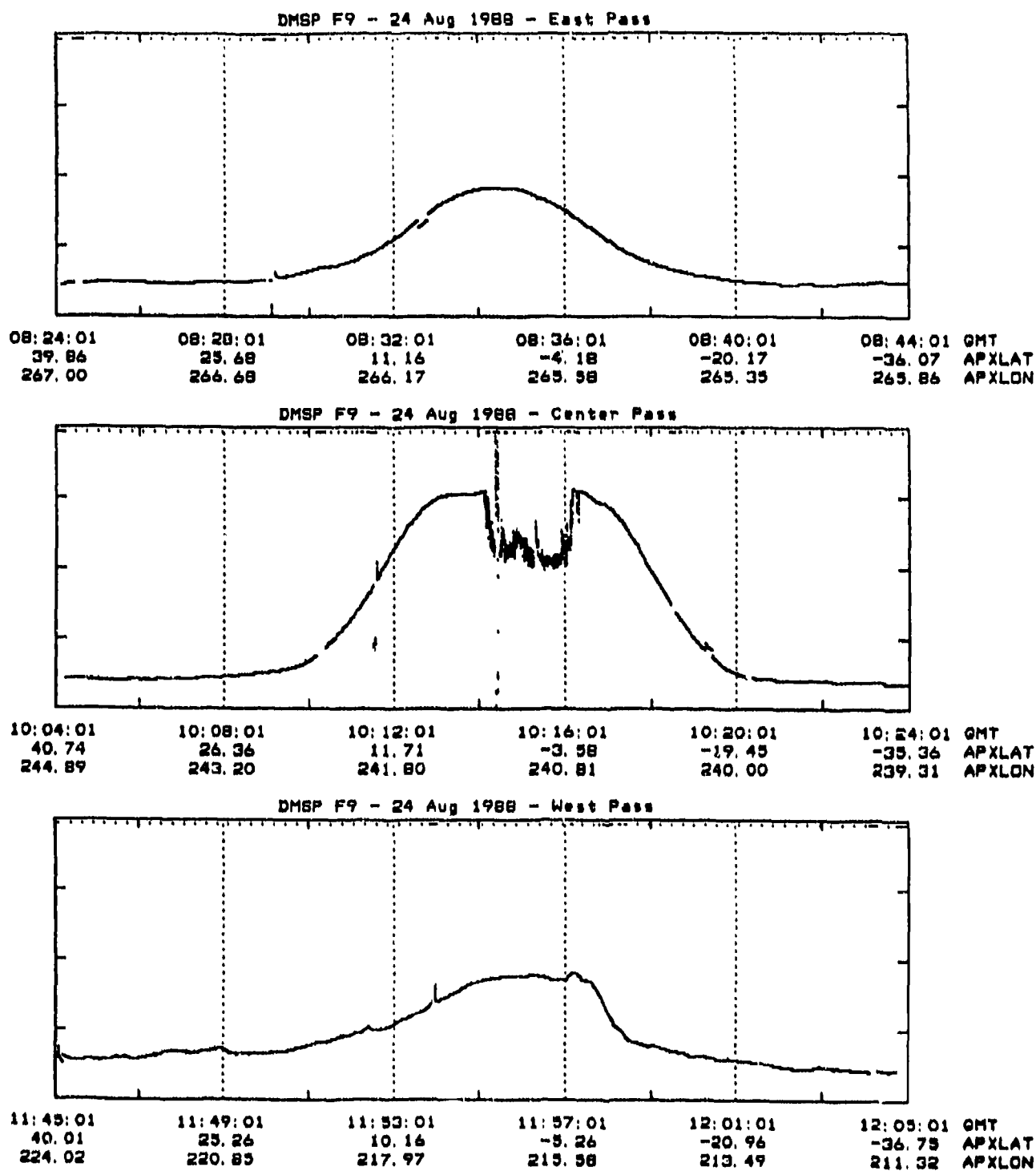


Figure 5. Total ion density measured by the SSIES/SM sensor on DMSP F8 near Kwajalein on 24 August 1988. The y-axis is ion density, ranging from 0.0 to 2.0×10^5 ; and the x-axis labels are GMT for Greenwich Mean Time (HH:MM:SS), APXLAT for modified apex latitude, and APXLON for apex longitude.

5. Conclusion

The primary objective of this project was to assess the potential for using *in-situ* observations of the ionospheric plasma available from the DMSP SSIES sensor package to characterize the level of scintillation effects on transionospheric radio paths. Methods were developed for using the data in this fashion, and estimates were made of the accuracy of the parameters generated using these methods. Data from a multi-instrument data-collection campaign conducted near the EISCAT incoherent radar facility in the early-evening auroral region were analyzed to test these methods and assess the potential for their use. Data from a second campaign in the equatorial region were analyzed to assess the usefulness of the SSIES data in determining the presence of depletion-plume structures in the post-sunset/pre-midnight equatorial ionosphere.

The methods developed for calculating irregularity/scintillation parameters from the SSIES observations require information not directly available from the SSIES data set, in particular the shape of the plasma density irregularities being sampled (the irregularity axial ratios) and the height variation of the irregularity strength. If these data are to be used operationally, the missing information must be provided either from direct observations or from models. As it is highly unlikely that observations of either the irregularity shapes or the height variation of the irregularity strength will be available for operational use, models must be used to provide this information.

A model for the shape of the irregularities is available from the WBMOD scintillation model, and while it provides reasonable estimates for the axial ratio parameter a (specifying the elongation of irregularities along the geomagnetic field), there is some concern about the estimates provided for axial ratio parameter b (specifying the presence and severity of elongation across the geomagnetic field direction)^[16]. Parametric studies^[7] showed that the irregularity-parameter estimates calculated from the SSIES data are very sensitive to changes in b , with errors as high as a factor of two in cases where this parameter was set to specify rod-like irregularities ($b = 1$) when in fact cross-field elongated sheet-like irregularities were present ($b > 1$). Further work should be done to improve these models.

A simple model was developed for the height variation of the irregularity strength ($\Delta N(h)$). This model was based on the assumption that the relative irregularity strength ($\Delta N/N$) is invariant with height and uses a two-component diffusive-equilibrium model of the electron density variation in the topside ionosphere^[13] to provide the height variation of N . An effective layer-thickness parameter (L_{eff}) is calculated from the $\Delta N(h)$ model and is used to scale the *in-situ* measurement of the irregularity strength (C_k) to an integrated measure ($C_k L$) which characterizes the entire layer. This scaling process is very sensitive to the ratio of the plasma density at the satellite to that at the F2 layer peak, and less so to details of the height variation in the topside. As there will be a fair measure of the density at the satellite from the SSIES data, it is imperative that an accurate measure (observation or model) of the F2 peak density consistent with the density at the satellite be available.

The results of the high-latitude assessment campaign were positive, but they were not conclusive due to problems with the phase scintillation observations on the AIO-AFSAT radio link. Estimates made of the intensity scintillation parameter, S_4 , from the SSIES observations matched the observed S_4 derived from the AIO-AFSAT intensity data well, doing better than the WBMOD climatological estimates generated throughout the pass analyzed. These promising indications that the data may be useful in the auroral region need to be confirmed by similar analysis of data collected in a repeat campaign conducted in January 1990.

There is less certainty of the usefulness of these data in the nighttime equatorial region. Intense scintillation in this region is dominated by depletion-plume structures, so for the data to be of operational use these structures must either be directly observed by the satellite passing through them or their presence must be inferred at some level of confidence from observations of the ambient plasma outside the plumes. A earlier study^[15] showed that the DMSP orbit is ill-suited for direct observation of these plumes due to the inclination of the orbit and the elongation of the plumes along the geomagnetic meridian. Because of this, there is a significant probability that the satellite may pass between plume structures without observing them. The current study confirmed this finding and provided some support to an assertion in the previous study that it may be possible to infer the presence of plumes based on a threshold effect in the absolute level of the electron density at the satellite altitude. This study was too limited to confirm this assertion or to establish either the threshold level or the degree of confidence one might have in predictions made of plume presence based on this threshold. With several years of SSIES data, however, it may be possible to address this issue and resolve it. This is planned for a follow-on effort.

No attempt was made in this study to assess the accuracy of the SSIES scintillation estimates in locations and local times other than the auroral region in the early evening hours and the equatorial region at night. Assessments should be made at other latitudes and local times, particularly in the polar cap and at mid-latitudes, as it is planned to use $C_{\text{p}}L$ values calculated from the SSIES observations to provide near real-time updates to the WBMOD model^[17]. Possible sources of scintillation data for assessments in other areas include routine and campaign measurements made by GL at the Thule geople station, measurements made by the prototype TISS (TransIonospheric Sounding System) receiver in the Shetland Islands, and the extensive HiLat/Polar BEAR data sets. It is hoped to include these assessments in the follow-on effort.

In all, the results of this project were generally positive. Methods were developed to use the SSIES data to characterize transionospheric scintillation effects, methods which appear to give reasonable results in the auroral region. While the results are not so clear in the equatorial region, there may be ways in which the SSIES data may be used indirectly to infer the presence of plume structures which cause the highest levels of scintillation encountered anywhere in the world. Further work is required, but the potential is there for using these data to improve the specification of worldwide scintillation levels.

REFERENCES

- [1] Fremouw, E. J. and Lansinger, J. M., *A Computer Model for High-Latitude Phase Scintillation Based on WIDEBAND Satellite data From Poker Flat*, DNA Report 5685F, Defense Nuclear Agency, Washington, DC, February 1981.
- [2] Secan, J. A., E. J. Fremouw, and R. E. Robins, "A review of recent improvements to the WBMOD ionospheric scintillation model," in *The Effect of the Ionosphere on Communications, Navigation, and Surveillance Systems*, edited by J. Goodman, Naval Research Laboratory, Washington, DC, 607-616, 1987.
- [3] Basu, Su., Basu, S., Weber, E. J., and W. R. Coley, "Case study of polar cap scintillation modeling using DE-2 irregularity measurements at 800 km," in *The Effect of the Ionosphere on Communications, Navigation, and Surveillance Systems*, edited by J. Goodman, Naval Research Laboratory, Washington, DC, 599-606, 1987.
- [4] Rino, C. L., "A power law phase screen model for ionospheric scintillation, 1. Weak scatter," *Radio Sci.*, 14, 1135-1145, 1979.
- [5] Holt, B. J., *Drift Scintillation Meter*, AFGL-TR-84-0103, Air Force Geophysics Laboratory, Hanscom AFB, MA, March 1984, ADA142523.
- [6] Greenspan, M. E., P. B. Anderson, and J. M. Pelagatti, *Characteristics of the Thermal Plasma Monitor (SSIES) for the Defense Meteorological Satellite Program (DMSP) Spacecraft S8 Through S10*, AFGL-TR-86-0227, Air Force Geophysics Laboratory, Hanscom AFB, MA, October 1986, ADA176924.
- [7] Secan, J. A., *An Assessment of the Application of In Situ Ion-Density Data From DMSP to Modeling of Transionospheric Scintillation, Scientific Report No. 1*, AFGL-TR-87-0269, Air Force Geophysics Laboratory, Hanscom AFB, MA, September 1987, ADA188919.
- [8] Secan, J. A. and R. M. Bussey, *An Assessment of the Application of In Situ Ion-Density Data From DMSP to Modeling of Transionospheric Scintillation, Scientific Report No. 2*, AFGL-TR-88-0280, Air Force Geophysics Laboratory, Hanscom AFB, MA, September 1988, ADA202415.
- [9] Secan, J. A. and L. A. Reinleitner, *An Assessment of the Application of In Situ Ion-Density Data From DMSP to Modeling of Transionospheric Scintillation, Scientific Report No. 3*, AFGL-TR-89-0264, Air Force Geophysics Laboratory, Hanscom AFB, MA, September 1989.
- [10] Secan, J. A., *Use of Apex Coordinate Transformation Tables*, NWRA-CR-87-R020, Northwest Research Associates, Inc., Bellevue, WA, 1987.

- [11] VanZandt, T. E., W. L. Clark, and J. M. Warnick, "Magnetic apex coordinates: a magnetic coordinate system for the ionospheric F2 layer," *J. Geophys. Res.*, 77, 2406-2411, 1972.
- [12] Rino, C. L. and E. J. Fremouw, "The angle dependence of singly scattered wavefields," *J. Atmosph. Terr. Phys.*, 39, 859-868, 1977.
- [13] Secan, J. A., *Development of Techniques for the Use of DMSP SSIE Data in the AWS 4D Ionosphere Model*, AFGL-TR-85-0107(1), Air Force Geophysics Laboratory, Hanscom AFB, MA, April 1985, ADA176412.
- [14] Weber, E. J., Private communication, 1990.
- [15] Young, E. R., W. J. Burke, F. J. Rich, and R. C. Sagalyn, "The distribution of topside spread F from *in-situ* measurements by Defense Meteorological Satellite Program: F2 and F4," *J. Geophys. Res.*, 89, 5565-5574, 1984.
- [16] Fremouw, E. J., J. A. Secan, and J. M. Lansinger, *Anisotropy Effects on and Other Characteristics of High-Latitude Scintillation*, DNA-TR-88-77, Defense Nuclear Agency, Washington, DC, December 1989.
- [17] Secan, J. A., M. P. Baldwin, and L. A. Reinleltner, *Real-Time Scintillation Analysis System, Technical Description*, NWRA-CR-89-R049, Northwest Research Associates, Inc., January 1990.
- [18] Bilitza, D., "The Atmospheric Explorer C ionospheric temperatures, dependences and representation," *Report UAG-90*, World Data Center for Solar-Terrestrial Physics, Boulder, CO, 114-122, May 1984.
- [19] Llewellyn, S. K. and R. Bent, *Documentation and Description of BENT Ionospheric Model*, AFGL-TR-73-0657, Air Force Geophysics Laboratory, Hanscom AFB, MA, 1973, AD772733.
- [20] Damon, T. D. and F. R. Hartranft, *Ionospheric Electron Density Model*, Tech. Memo 70-3, Aerospace Environmental Support Center, Ent AFB, CO, July 1970 (available from the USAF Air Weather Service Technical Library, Scott AFB, IL, 62225).
- [21] Flattery, T. W. and A. C. Ramsay, "Derivation of total electron content for real time applications," in *Effect of the Ionosphere on Space Systems and Communications*, edited by J. Goodman, Naval Research Laboratory, Washington, DC, 336-344, 1975.

Appendix. Topside Electron Density Model

The electron density profile model used in this study was developed specifically for use with the DMSP SSIES sensor package^[13]. The underlying structure of the topside section of the model is that of a two-component ionosphere (O+ and H+) in diffusive equilibrium, but it has been parameterized to allow the model to be fit to non-equilibrium conditions. Assuming charge neutrality, the electron density profile will be identical to the height variation of the ionospheric plasma density, which for this model is given by

$$N_e(h) = N_p(h) = \left(\frac{T_{p0}}{T_p} \right) e^{\beta \mu} \left[N_o(O+) e^{-16\alpha I} + N_o(H+) e^{-I} \right] \quad [A-1]$$

$$\alpha = \alpha_0 + \alpha_1 (h-400) \quad [A-2]$$

where T_p is the plasma temperature ($T_i + T_e$); T_{p0} is the plasma temperature at a reference height (h_0); $N_o(O+)$ and $N_o(H+)$ are the number densities of O+ and H+ at the reference height; α_0 , α_1 , and β are profile adjustment parameters; and μ and I are integral functions given by

$$\mu(h) = \int_{h_0}^h \left(\frac{T_e}{T_i} \right) \left(\frac{m_+ g}{k T_p} \right) \left(\frac{16+R}{1+R} \right) dh \quad [A-3]$$

$$I(h) = \int_{h_0}^h \left(\frac{m_+ g}{k T_i} \right) dh \quad [A-4]$$

where m_+ is the mass of H+, and R is defined as the ratio of $N(H+)$ to $N(O+)$. Ion and electron temperatures are obtained from a recent model based on an analysis of data from the AE-C satellite^[18]. The density ratio, R , is based on the O+ to H+ transition height, h_T , defined as the height at which $N(O+) = N(H+)$. This parameter can be either (1) calculated from observations of $N(O+)$, $N(H+)$, and T_p from the SSIES RPA sensor, or (2) obtained from an empirical model of h_T derived from published analyses of topside profiles from the Alouette satellites and RPA data from OGO-6^[13].

The topside model is fit to the F2 peak by means of a parabolic layer taken from the Bent profile model^[19] of the form

$$N_e(h) = N_{mF2} \left[1 - \left(\frac{h - h_{mF2}}{Y_t} \right)^2 \right] \quad [A-5]$$

where N_{mF2} and h_{mF2} are the density and height of the F2 layer peak, and Y_t is the parabolic semi-thickness. The Y_t parameter can be either (1) estimated in the procedure used to fit the profile to observations, or (2) obtained from the expressions used in the original Bent model. Equations [A-1] and [A-5] are fit together at the height where the plasma scale height calculated from the two representations of $N_p(h)$ are equal. This must be calculated iteratively, but rarely requires more than four or five iterations. This height is also used as the reference height, h_o , for the parameters in Equation [A-1].

For the sake of providing a complete plasma density profile, the bottomside section of the Air Weather Service (AWS) RBTEC model is used to describe the height variation below the F2 peak^(20,21). This model uses three Chapman-function layers to describe the three main ionospheric layers (E, F1, and F2). The choice of models for the bottomside of the profile has little impact on the present study, as the irregularity layer is assumed to start either at or just slightly below the F2 peak.